IL NUOVO CIMENTO **45 C** (2022) 57
DOI 10.1393/ncc/i2022-22057-0

Colloquia: IWM-EC 2021

Study of the Hoyle state in ^{12}C produced by ^{20}Ne + ^{12}C reactions

A. Rebillard-Soulié(1), D. Gruyer(1) and G. Verde(2)(3) for the FAZIA Collaboration(1)(2)(3)(4)(5)(6)(7)(8)(9)(10)(11)(12)(13)(14)(15)(16)(17)
(FAZIACOR Experiment)

(1) *Normandie Université, ENSICAEN, UNICAEN, CNRS/IN2P3, LPC Caen - Caen, France*
(2) *Laboratoire des 2 Infinis (L2IT-IN2P3) - Toulouse, France*
(3) *INFN, Sezione di Catania - 64 Via Santa Sofia, I-95123, Catania, Italy*
(4) *Center for Extreme Nuclear Matters (CENuM), Korea University - Seoul 02841, Republic of Korea*
(5) *Departamento de Ingeniería Eléctrica y Centro de Estudios Avanzados en Física, Matemáticas y Computación, Universidad de Huelva - 21007 Huelva, Spain*
(6) *Dipartimento di Fisica e Astronomia, Università di Firenze - Via G. Sansone 1, 50019 Sesto Fiorentino (FI), Italy*
(7) *Department of Physics, Inha University - Incheon 22212, Republic of Korea*
(8) *Department of Physics, Korea University - Seoul 02841, Republic of Korea*
(9) *Department of Science Education, Ewha Womans University - Seoul 03760, Republic of Korea*
(10) *Faculty of Physics, Astronomy and Applied Computer Science, Jagiellonian University 30-348 Kracow, Poland*
(11) *Grand Accélérateur National d'Ions Lourds (GANIL), UAR 3266, CEA-DRF/CNRS-IN2P3 - Boulevard Henri Becquerel, F-14076 Caen Cedex, France*
(12) *Heavy Ion Laboratory, University of Warsaw - 02-093 Warszawa, Poland*
(13) *INFN, Laboratori Nazionali di Legnaro - Viale Dell'Università 2, 35020, Legnaro, Italy*
(14) *INFN Laboratori Nazionali del Sud - Via S. Sofia 62, 95125 Catania, Italy*
(15) *INFN Sezione di Firenze - 50019 Sesto Fiorentino (FI), Italy*
(16) *INFN Sezione di Padova - 35131 Padova, Italy*
(17) *Université Paris-Saclay, CNRS/IN2P3, IJCLab - 91405 Orsay, France*

received 12 May 2022

Summary. — Since its discovery, the Hoyle state of ^{12}C has attracted much interest. Its properties have been discussed several times, due to its cluster structure and the astrophysical implications. In this contribution, the Hoyle state decay has been studied using ^{20}Ne+^{12}C reactions at 25 MeV/nucleon. The invariant mass method has been used to get all the properties of the original ^{12}C starting from a 3-α correlation. The background in the reconstructions was removed using the event mixing method. Finally, we made a simulation of the 3-α decay, including the effects of angular and energy resolutions assuming different possible modes. As a first result, we show a qualitative agreement of the experimental data with the simulated sequential decay. Further studies are ongoing to precisely extract the branching ratios and all the uncertainties due to the simulation parameters.

1. – Introduction

In 1953, Hoyle showed that the cross section of the triple-α process at star temperatures is too small to explain the observed abundance of stable ^{12}C in the universe [1]. He stated that there must be a resonance close to the $^{8}\mathrm{Be} + \alpha$ threshold boosting the reaction rate of this process: the Hoyle state of ^{12}C ($E_x = 7.654\,\mathrm{MeV}$). This state has been first observed in 1953 by Dunbar *et al.* [2], then more precisely in 1957 by Cook *et al.* [3]. The formation of excited ^{12}C is then achieved in a two-step process: first by the formation of a ^{8}Be in its ground state with two α (eq. (1a)), and then by the capture of a third α leading to the Hoyle state of ^{12}C (eq. (1b)). The excited nucleus can finally decay radiatively to form a stable ^{12}C with a very small probability. Consequently, the decay properties of this state play an important role in the production of ^{12}C.

$$\alpha + \alpha \rightleftharpoons {}^{8}\mathrm{Be}, \tag{1a}$$

$$^{8}\mathrm{Be} + \alpha \rightleftharpoons {}^{12}\mathrm{C}^{*} \rightarrow {}^{12}\mathrm{C} + \gamma. \tag{1b}$$

The structure of the Hoyle state has also been described in terms of α clusters. In this respect, different theoretical approaches have been developed [4-8]. They all predict a three α-particle structure in several geometric arrangements: isosceles or equilateral triangle, linear chain, etc. The way the Hoyle state will decay may carry signals of its initial arrangement.

The Hoyle state can decay non-radiatively according to four different modes:

- Sequential decay (SD), in which a first α particle is emitted forming a ^{8}Be in ground state. Then, the ^{8}Be decays into two α.
- Full phase-space direct decay (DDΦ) with an equiprobable population of the three-body phase-space available to the α particles. It may correspond to a gas-like state.
- Equipartition direct decay (DDE), in which the three α share the same amount of kinetic energy. This mode has been associated to a possible Bose-Einstein Condensate (BEC-like structure) [9].
- Linear direct decay (DDL) in which one α is at rest and the other two are emitted in opposite directions. It may result from a linear chain structure of the 3 α particles in the Hoyle state.

Several studies have attempted to evaluate the different branching ratios of these modes [10-15]. Most of them point to a contribution of direct decay close or consistent with zero. A recent study by Raduta *et al.* [9], performed on heavy-ion fragmentation reactions, revealed a much larger proportion of direct decay modes (about 17%). This last result seems to contradict other published studies. Such a result may have important consequences for the 3-α process in stars as well as for the existence of a Bose-Einstein condensate in α-cluster states.

Motivated by the above observations, in this paper we develop a new approach to probe the decay of the Hoyle state. Using an analysis of the detected particles and a Monte Carlo simulation of the decay, the different decay modes will be studied and compared. The high performance FAZIA (Forward A and Z Identification Array) multi-detector [16-20] is used to probe multi-particle correlations which are necessary for the ^{12}C Hoyle state reconstruction.

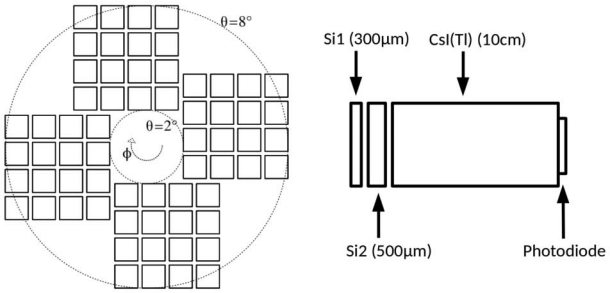

(a) (b)

Fig. 1. – Geometry of the FAZIA multidetector in its 4 blocks configuration (a) and layout of a telescope (b).

2. – Experimental setup

The experiment was performed at the LNS in Catania (Italy) using the FAZIA multi-detector in order to precisely identify in charge and mass the detected charged particles. Its high granularity leads to a good reconstruction of excited parent nuclei decaying via multi-particle correlations.

In this experiment, FAZIA consisted of four blocks (as shown in fig. 1(a) [21]), with each of these blocks including sixteen telescopes (having an entrance window of $2\times2\,\mathrm{cm}^2$). Each FAZIA telescope consists of three detection stages: silicon 1 ($300\,\mu$m); silicon 2 ($500\,\mu$m); CsI(Tl) (10 cm) as shown in fig. 1(b). The angular coverage range is from about 2° to 8° and the isotopic identification goes up to $Z \simeq 25$ for the ΔE-E method and $Z \simeq 20$ for the pulse-shape analysis in silicon stages [22-25]. For this study, we analyze the reactions from a ^{20}Ne at 25 MeV/nucleon beam impinging on a $0.2\,\mu\mathrm{g/cm}^2$ thick ^{12}C target.

3. – Analysis

3˙1. ^{12}C *reconstruction.* – In order to reconstruct the excited ^{12}C, we selected all events with at least three identified α particles and we used the invariant mass method to compute its properties. In fig. 2, we can see the correlations between reconstructed excitation and kinetic energy of the 3-α system for the selected events.

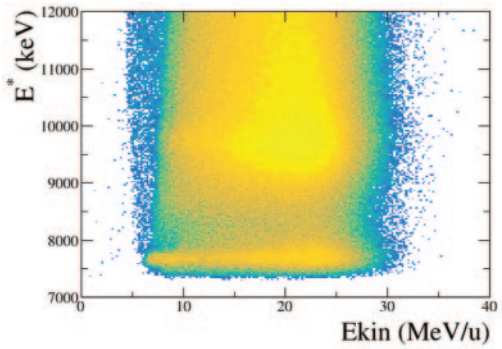

Fig. 2. – E^*-E_{kin} correlation for the 3-α system.

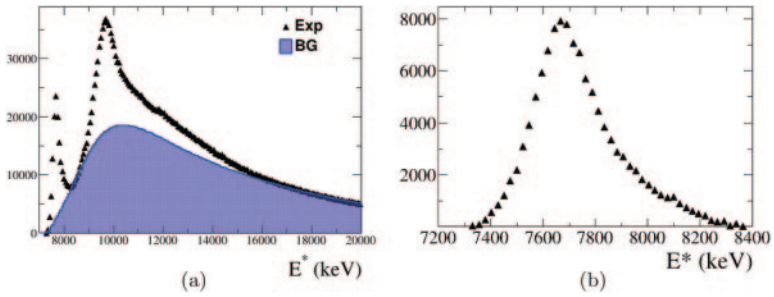

Fig. 3. – Excitation energy spectrum of the reconstructed ^{12}C for coincidences (in black markers) and event mixing (in blue filled) (a). Excitation energy spectrum from 7.2 MeV to 8.4 MeV after background treatment (b).

3˙2. *Background treatment and kinematic weighting.* – Figure 3(a) shows the excitation energy (E^*) distribution in which two peaks are visible: one around 7.6 MeV (0_2^+ Hoyle state) and a broader one around 10 MeV. A large part of counts in fig. 3 does not originate from the decay of ^{12}C, thus leading to a background component. This background has been evaluated using an "event mixing" technique. This method consists of taking three α's from three different events of the same subset as for the coincidence reconstructions (*i.e.*, events with at least 3 α particles identified). In this way, we generate an estimate of the background component.

The kinematic properties (polar angle θ and kinetic energy E_{kin} distributions of the ^{12}C) of uncorrelated reconstructions should reproduce the correlated ones. Therefore, these uncorrelated reconstructions are weighted according to the ratio between the yields of coincidence and uncorrelated spectrum $Y(E_{kin}, \theta)$ as in eq. (2),

$$w(E_{kin}, \theta) = \frac{Y_{coinc}(E_{kin}, \theta)}{Y_{BG}(E_{kin}, \theta)} \tag{2}$$

The background component of the excitation energy spectrum is presented as a shaded area histogram in fig. 3(a), while fig. 3(b) shows the excitation energy distribution centered on the Hoyle state peak after background subtraction. We then choose a gate around the Hoyle state peak (7.5–7.8 MeV) for the remainder analysis.

3˙3. *Simulated events.* – We built a simulation of the Hoyle state decay where all detection effects are carefully taken into account. We first generated excited ^{12}C nuclei with similar kinematic properties as in the experimental data. Then, we defined the different decay modes as it is shown in fig. 4. Events are generated according to each mode, by applying the proper energy and angular distributions on the emitted α particles.

A first effect of the detection is applied to all the simulated events by taking into account the angular resolution of the FAZIA telescopes, as well as identification thresholds, pile-up effects, etc., profiting from the KaliVeda analysis framework [26].

3˙4. *Energy resolution.* – The measurement of the energy loss in each detection stage is characterized by a certain resolution depending on the energy and the type of the detection stage (Si, CsI). We assume here the following form:

$$\sigma E_i = a_i \times \sqrt{E_i} + b_i \tag{3}$$

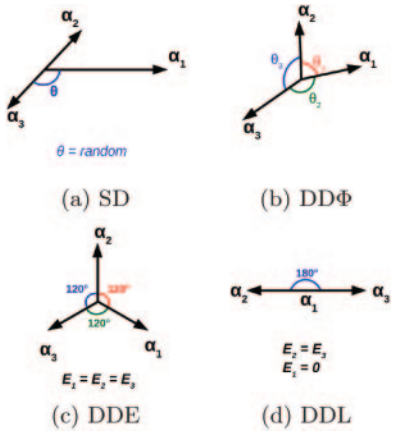

Fig. 4. – Scheme of the different decay modes. Relative angles and energies of the α's are represented.

where i = Si1, Si2, CsI. The first term of eq. (3) accounts for the fluctuations in the charge carriers creation and collection (following a Poisson distribution), while the constant term accounts for the resolution of the electronic chain.

The a_i and b_i parameters have to be adjusted for each type of detection stage: a_{Si1}, a_{Si2}, b_{Si1}, b_{Si2}, a_{CsI}, b_{CsI}. We assume here that $a_{Si1} = a_{Si2} = a_{Si}$. The b_{Si1} parameter can be fixed using 3-α source spectrum (^{239}Pu, ^{241}Am, ^{244}Cm). The electronic chain of the low gain channel of FAZIA Si1 is the same as the Si2 one. We then determine b_{Si2} from the α resolution on Si1 low gain channel. We finally end with only three free parameters: a_{Si}, a_{CsI} and b_{CsI}.

A χ^2 minimization of the E^* spectrum is achieved to find the optimum values for the 3 above resolution parameters. In fig. 5 we show the excitation energy spectrum with the different resolution effects compared to the experimental spectrum. The highest energy

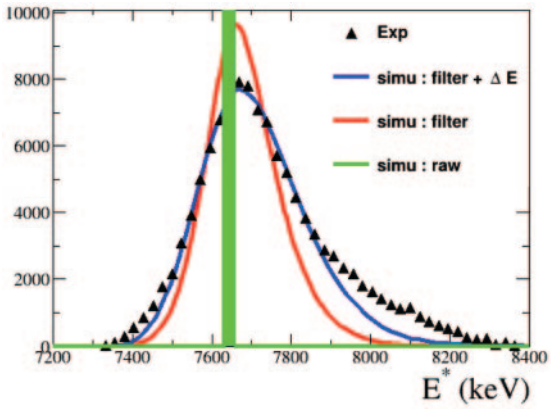

Fig. 5. – Excitation energy spectra for experimental data (black markers) and each step of the simulation: raw (green line), angular resolution (red line) and angular + energy resolution (blue).

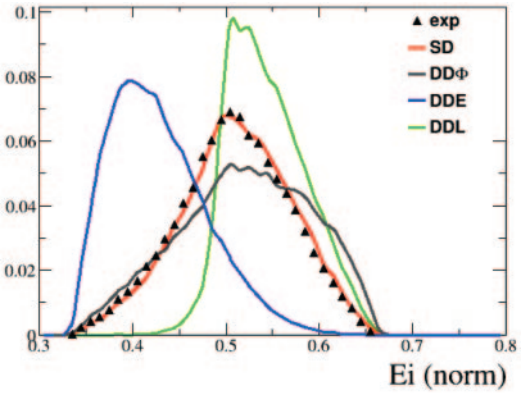

Fig. 6. – E_i spectrum for each decay modes: sequential decay (red); full phase-space direct decay (grey); equipartition direct decay (blue); linear direct decay (green). Data points are in black markers.

among the 3 α in the center of mass reference frame (E_i) is the observable we choose to discriminate between the different decay modes. In fig. 6 we present the different E_i spectra for all decay modes compared to the experimental one with the optimal resolution parameters. A good agreement of the experimental data with the sequential decay spectrum is visible. More advanced analysis has to be done to properly estimate the contributions of the different modes and the associated uncertainties.

4. – Conclusion

In this study, we initiated an analysis of the Hoyle state decay. The $^{20}\mathrm{Ne} + {}^{12}\mathrm{C}$ at 25 MeV/nucleon reaction was used to populate the Hoyle state. The produced α particles have been detected using four FAZIA blocks. The 3-α correlation analysis was used to reconstruct the excited ^{12}C. An estimation of the uncorrelated background has been done by an event mixing method. Finally, a Monte Carlo simulation was made to generate different decay modes considering also the experimental resolutions. We showed a good agreement of the simulated sequential decay with data. A further study will be published on the proper estimation of the direct decay branching ratio with an optimization of the simulation parameters.

* * *

The author would like to thank the Superconducting Cyclotron staff of LNS, for providing a very high quality beam. The support of the Machine shop team of LNS is also gratefully acknowledged. The author gives special thanks to S. Barlini, B. Borderie, R. Bougault, A. Camaiani, C. Ciampi, J. Frankland, D. Gruyer, N. Le Neindre, S. Piantelli and G. Verde for contributing to the corrections of the present paper.

REFERENCES

[1] Hoyle F., *Astrophys.J. Suppl. Ser.*, **1** (1954) 121.
[2] Dunbar D. N. F. *et al.*, *Phys. Rev.*, **92** (1953) 649.
[3] Cook C. W. *et al.*, *Phys. Rev.*, **107** (1957) 508.
[4] Margenau H., *Phys. Rev.*, **59** (1941) 37.

[5] Brink D. and Boeker E., *Nucl. Phys. A*, **91** (1967) 1.
[6] Tohsaki A. *et al.*, *Phys. Rev. Lett.*, **87** (2001) 192501.
[7] Smith R. *et al.*, *Few-Body Syst.*, **61** (2020) 14.
[8] Kanada-En'yo Y. and Horiuchi H., *Prog. Theor. Phys. Suppl.*, **142** (2001) 205.
[9] Raduta A. *et al.*, *Phys. Lett. B*, **705** (2011) 65.
[10] Grenier F. *et al.*, *Nucl. Phys. A*, **811** (2008) 233.
[11] Dell'Aquila D. *et al.*, *Phys. Rev. Lett.*, **119** (2017) 132501.
[12] Freer M. and Fynbo H., *Prog. Part. Nucl. Phys.*, **78** (2014) 1.
[13] Freer M. *et al.*, *Phys. Rev. C*, **49** (1994) R1751.
[14] Kirsebom O. S. *et al.*, *Phys. Rev. Lett.*, **108** (2012) 202501.
[15] Manfredi J. *et al.*, *Phys. Rev. C*, **85** (2012) 037603.
[16] Barlini S. *et al.*, *J. Phys.: Conf. Ser.*, **1561** (2020) 012003.
[17] Bougault R. *et al.*, *Eur. Phys. J. A*, **50** (2014) 47.
[18] Valdré S. *et al.*, *Nucl. Instrum. Methods A*, **930** (2019) 27.
[19] Casini G. *et al.*, *EPJ Web of Conferences*, **66** (2014) 11006.
[20] Frosin C. *et al.*, *Nucl. Instrum. Methods Phys. Res. Sect. A*, **951** (2020) 163018.
[21] Camaiani A. *et al.*, *Phys. Rev. C*, **103** (2021) 014605.
[22] Gruyer D. *et al.*, *Nucl. Instrum. Methods Phys. Res. Sect. A*, **847** (2017) 142.
[23] Gruyer D., *Nuovo Cimento C*, **41** (2018) 166.
[24] Le Neindre N. *et al.*, *Nucl. Instrum. Methods Phys. Res. Sect. A*, **701** (2013) 145.
[25] Pastore G. *et al.*, *Nucl. Instrum. Methods Phys. Res. Sect. A*, **860** (2017) 42.
[26] KaliVeda Data Analysis Framework, `http://indra.in2p3.fr/kaliveda`.